

DOI: 10.15825/1995-1191-2025-1-135-144

# INVESTIGATION OF THE HISTOARCHITECTURE OF BOVINE PERICARDIUM AS THE PRIMARY MATERIAL USED IN RECONSTRUCTIVE SURGERY AND BIOPROSTHESIS

A.I. Zvyagina<sup>1</sup>, K.V. Pyatina<sup>1</sup>, V.V. Minaiychev<sup>1</sup>, M.I. Kobayakova<sup>1</sup>, Ya.V. Lomovskaya<sup>1</sup>, A.S. Senotov<sup>1</sup>, A.Yu. Teterina<sup>2</sup>, I.S. Fadeeva<sup>1</sup>

<sup>1</sup> Institute of Theoretical and Experimental Biophysics, Moscow, Russian Federation

<sup>2</sup> Baikov Institute of Metallurgy and Materials Science, Moscow, Russian Federation

**Objective:** to study the composition and topology of the extracellular matrix (ECM) of bovine pericardium and to identify the best tissue areas suitable for the fabrication of bioprosthetic heart valves (BHVs). **Materials and methods.** The pericardium samples of healthy sexually mature bulls were studied; the native pericardium was divided into three experimental groups: core tissue (BP-CT group), heart base (BP-HB) and connective ligament base (BP-CL). Scanning electron microscopy was used to examine the structure of the pericardial surfaces (*p. serosum* and *p. fibrosum*), while differential histochemical analysis was used to study the topology of various pericardial regions, with identification and quantification of the main constituents of the extracellular matrix (ECM) (collagen, elastin, lipids, and glycosaminoglycans). Quantification was performed by bioimaging and digital analysis of histological images using the ImageJ software. **Results.** The BP-CT group had the lowest cellular density and, consequently, DNA content ( $369.75 \pm 23.12$  ng/mg), in addition to having the most homogeneous, predominantly collagenous ( $95.6 \pm 2.9\%$ ) matrix composition with minimal lipid ( $2.6 \pm 1.5\%$ ), glycosaminoglycan ( $0.68 \pm 0.7\%$ ) and elastin ( $3 \pm 2.4\%$ ) content. The BP-CL group had the highest levels of elastin and glycosaminoglycans ( $27.8 \pm 3\%$  and  $17.5 \pm 0.6\%$ , respectively), while the BP-HB group had the highest lipid content ( $21.2 \pm 2.7\%$ ). On the *p. serosum* side, the ECM composition was noticeably homogeneous, while elastin fibers, glycosaminoglycans, and lipid clusters were predominantly found on the *p. fibrosum* side, indicating the natural polarity of the material, which should be considered when fabricating biomaterials. **Conclusion.** The findings in this study revealed that bovine pericardial topology varied depending on the tissue area. Only the main pericardial tissue can be used to create BHVs, as evidenced by the comparative homogeneity of ECM composition and relatively low cellular density. The high content of elastin, glycosaminoglycans and lipids in specific pericardial tissue areas (the BP-HB and BP-CL groups) suggests that either this layer needs to be removed more thoroughly during implant fabrication (e.g., by selective purification techniques) or these pericardial tissue areas should be used where heterogeneity of the composition is desired (e.g., in maxillofacial and orthopedic surgery).

**Keywords:** bovine xenopericardium, pericardial topology, extracellular matrix, bioprosthetic heart valves, calcification.

## INTRODUCTION

Xenogenic serous membranes are increasingly used as a base for developing a wide range of implantable biomaterials [1]. Among them, bovine xenopericardium (BP) – which undergoes fixation, decellularization, and delipidization – is one of the most commonly used biomaterials in modern cardiovascular surgery [2].

BP serves as the primary material for various bioprostheses and auxiliary cardiovascular implants, including bioprosthetic heart valves (BHVs), venous and arterial conduits, cardiovascular patches, and sutures [1, 3, 4]. However, a major challenge with BP-based biomaterials is their susceptibility to calcification within the recipient's body, significantly limiting implant lon-

gevity. Addressing this issue remains a critical priority in reconstructive cardiovascular surgery [5–7].

At the same time, it is known that the composition of the pericardial extracellular matrix (ECM) can influence the body's general tissue and cellular response to an implanted material [8, 9]. For example, it has been shown that pericardial basal membrane proteins positively influence human aortic endothelial cell migration, adhesion, proliferation, inflammatory response, and laminin production, which in turn contributes to one of the most important indicators of BHV biointegration – reendothelization. Moreover, emerging data suggest that the propensity of BHVs to calcification may also be influenced by the composition of the pericardial ECM. Elastin fibers, for instance, are well-known biomaterial

**Corresponding author:** Alena Zvyagina. Address: 3, Institutskaya str., Pushchino, 142290, Russian Federation. Phone: (960) 600-93-00. E-mail: alennazvyagina@gmail.com

calcification sites [10, 11]. Elastin is a key structural protein that forms the framework of blood vessel walls (primarily arteries), the dermis, and interalveolar septa of the lungs. When damaged, it has been shown to accumulate calcium salts, becoming a site for medial calcification in several pathological conditions, including hyperphosphatemia (linked to kidney and endocrine disorders), diabetes and atherosclerosis, pseudoxanthoma elasticum, beta-thalassemia, monckeberg calcification, rheumatoid arthritis, Singleton–Merten syndrome, secondary hyperparathyroidism, Kawasaki disease, vitamin K deficiency (including warfarin-associated variant) and vitamin D metabolic disorders [10, 12]. A number of studies have also shown that degradation and fragmentation of elastin fibers in heart and vascular valve grafts are major contributors to aseptic calcification after implantation in the recipient's body [10–14].

Damaged (primarily sulfated) glycosaminoglycans (GAGs) play a crucial role in biomaterial calcification by acting as nucleation sites for calcium deposition in biomaterials [12]. Furthermore, the destruction of proteoglycans – which contain up to 95% GAGs and play a crucial role in collagen fiber stabilization – leads to the exposure of gap zones (H-zones) on collagen fibrils, facilitating the deposition of calcium phosphates directly within the ECM of biomaterials [15].

The significant role of these matrix components in BHV calcification is underscored by the ongoing development of anticalcification treatments aimed at stabilizing elastin and GAGs. Numerous studies have demonstrated that preserving GAGs and elastin effectively reduces BHV calcification, highlighting their potential as therapeutic targets [16–19].

In addition, cellular density is a key factor in donor tissue selection for biomaterial manufacturing, as cell membranes carry the primary antigens responsible for implant rejection [20]. This is particularly critical for BHVs, where, beyond immunological rejection, residual lipids from cell membranes can trigger passive aseptic calcification [21, 22].

Despite years of research into decellularization and delipidization techniques, complete lipid removal remains challenging. Achieving an optimal balance between effective lipid extraction and preservation of the biomaterial's structural and mechanical integrity is crucial [23].

Moreover, nuclear DNA, being one of the most resilient biomolecules, poses additional challenges in complete tissue clearance during decellularization. Residual DNA not only remains difficult to degrade but also serves as a phosphate source, further contributing to calcification [24].

Currently, there is an ongoing search for the optimal pericardial sites best suited for biomaterial production [2]. Studies have shown that BHV calcification patterns depend significantly on the type of donor tissue used in prosthesis fabrication [25]. In this context, it is essential to consider key donor tissue parameters – such as elastin, GAG content, lipid composition, and cellular density – when selecting pericardial tissue for BHV manufacturing. However, no such data currently exist for BP, with most guidelines focusing primarily on physical properties, such as biomechanical strength and elasticity, which are influenced by anisotropy and fiber orientation.

Given the lack of scientific literature detailing the histoarchitecture and biochemical composition of BP using differential histochemistry methods, this study conducted a comprehensive histochemical analysis of native BP. The goal was to identify tissue regions with the most homogeneous collagen composition, minimal elastin, GAG, and lipid content, and the greatest potential for use in BHV fabrication.

## MATERIALS AND METHODS

### Object of study

Pericardial samples were obtained from sexually mature, healthy bulls through the slaughterhouse of the Kaluga Niva APK meat processing plant (Torkotino village, Kaluga Oblast). All collected tissue was immediately placed in sterile 0.9% sodium chloride solution containing gentamicin (400 µg/mL) and fluconazole (50 µg/mL) within 30 minutes post-slaughter and transported to the laboratory in a thermocontainer maintained at 2–8 °C.

Upon arrival at the laboratory – no later than 4 hours post-slaughter and extraction – the pericardium was mechanically cleaned of adipose tissue and rinsed in 0.9% NaCl solution containing 5000 ED/100 mL heparin (Moscow Endocrine Plant, Russia) to remove blood residues.

After cleansing and rinsing the pericardial fragments free of heparin using sterile cold 0.9% sodium chloride solution, the samples were divided into three study groups based on tissue region (Fig. 1): the core tissue (BP-CT group), the heart base (BP-HB group), and the connective ligament base (BP-CL group).

### Scanning electron microscopy

The surface structure of lyophilized BP fragments (1 cm<sup>2</sup>) was then examined using scanning electron microscopy (SEM) (VEGA III, Tescan, Czech Republic). To ensure optimal surface preservation and prevent matrix component degradation, a matrix-preserving lyophi-

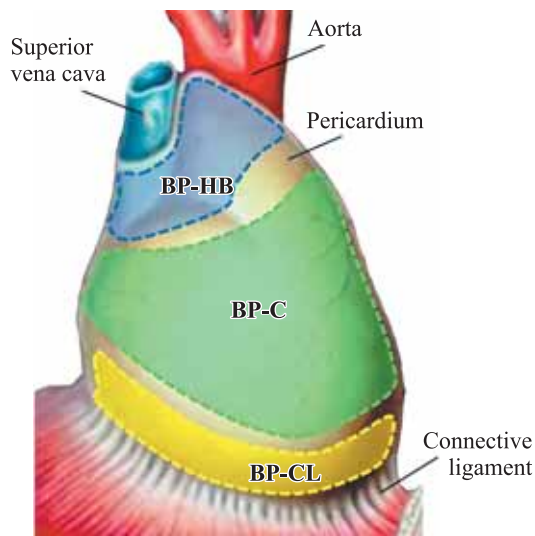


Fig. 1. Sampling areas of the studied fragments of the native pericardium. BP-HB, vessel base zone; BP-CT, main part of tissue; BP-CL, ligament base zone

lization process was employed. This included rapid deep freezing of tissue fragments in a Kelvenator laboratory freezer at  $-80\text{ }^{\circ}\text{C}$ , reaching the conditional eutectic point of  $-57\text{ }^{\circ}\text{C}$ , and lyophilization for 24 hours in freeze-drying flasks (FreeZone 2.5 Liter Benchtop Freeze Dry System, Labconco, Canada) while keeping samples suspended to prevent direct contact with flask surfaces.

After lyophilization, a conductive coating was applied to the surface of the studied fragments by sputtering gold particles using a vacuum atomizer Q150R ES (Quorum Technologies, England). For all examined fragments, the microrelief of both the serous (*p. serosum*) and fibrous (*p. fibrosum*) surfaces was analyzed.

### DNA quantification

To determine DNA content, 20 mg BP fragments were selected ( $n \geq 5$  per study group). Genomic DNA was isolated using the DNA-EXTRAN-2 kit (Syntol, Russia) following the manufacturer's instructions. The DNA concentration in the extracted solutions was measured using a NanoVue Plus spectrophotometer (Biochrom, USA) at a wavelength of 260 nm.

### Differential histologic analysis

To preserve the native structure of the BP extracellular matrix, cryotomy was employed to prepare histologic sections, preventing lipid washout, tissue shrinkage from dehydration, and structural matrix alterations. For this purpose: BP fragments were fixed in 10% buffered neutral formalin at  $22 \pm 2\text{ }^{\circ}\text{C}$  for at least 24 hours, excess phosphates were removed by washing with running water, samples were embedded in cryopreservation medium (O.C.T. Compound Tissue Tek, Sakura, Japan).

Sections  $9\text{ }\mu\text{m}$  thick were obtained using an MEV cryotome (SLEE Medical GmbH, Germany).

Histological preparations were stained using a combination of histological and differential histochemical stains, including: hematoxylin-eosin, Sudan III (lipid identification), Lilly trichrome (collagen detection), Verhoeff–Van-Gieson (elastin identification), and periodic acid-Schiff (PAS) & alcian blue (GAG detection) [26].

Micrographs and overview histotopograms of the stained preparations were captured using a Nikon Eclipse Ti-E microscopy station (Nikon, Tokyo, Japan).

### Histomorphometric analysis

Inverted microscope system Nikon Eclipse Ti-E (Nikon, Tokyo, Japan) was used in combination with the splicing method to generate high-resolution histotopograms of stained histological specimens. These images were processed using NIS Elements AR4.13.05 software (build 933, Nikon, Tokyo, Japan).

Histomorphometric analysis was conducted using ImageJ software (version 1.54h, NIH, Bethesda, MD, USA). Each group included a minimum of four histotopograms, with each histotopogram representing an average splice of  $35 \pm 15$  standard  $\times 4$  magnified images.

Bioimaging of micrographs was performed by superimposing color masks onto the images and calculating the area of the mask relative to the total sample slice within the field of view ( $2000 \times 2000\text{ }\mu\text{m}$ ). The proportion of collagen, elastin, lipids, and GAGs in each sample was quantified as a percentage of the total evaluated slice area.

### Statistical analysis

The study results are expressed as mean  $\pm$  standard deviation ( $M \pm SD$ ). Each experiment was conducted with at least four repetitions ( $n \geq 4$ ), and 16 fields of view per group ( $n = 16$ ) were analyzed for microscopic images. Statistical significance was assessed using one-way analysis of variance (ANOVA), followed by the Holm–Sidak multiple comparison test, with a significance threshold of  $p < 0.05$ . Data processing was performed using Python 3 (ver. 3.10.10) in the Spyder development environment (v. 5.4.1), utilizing the Pandas (v. 1.5.2), NumPy (v. 1.24.2), SciPy (v. 1.5.2) and SciPy (v. 1.10.0) libraries. Graphical representation of results was done using Seaborn (v. 0.12.2) and Matplotlib (v. 3.7.0).

## RESULTS AND DISCUSSION

For all groups, the microrelief of the *p. serosum* and *p. fibrosum* surfaces – critical structures of bioprosthesis

tissue that absorb the hydraulic shock of systemic blood flow – was thoroughly examined.

Thanks to the use of gentle lyophilization and cryotomy methods, a delicate, syrup-like GAG layer was observed on the surface of the collagen matrix in all study groups (Fig. 2). Comparative analysis revealed that on the *p. serosum* side, this layer was denser and smoother in the BP-HB and BP-CL groups than in the BP-CT group.

The presence of an intact GAG layer, which envelops collagen and elastin fibers susceptible to platelet aggregation and calcification, is a crucial factor in enhancing the durability and thromboresistance of BHVs.

No additional structural differences were observed among the studied groups using SEM.

Histochemical analysis of BP-CT group samples revealed that the primary pericardial matrix predominantly comprised wave-like collagen fibers (Fig. 3, a). The overall matrix architecture exhibited a porous structure with numerous cavities, which play a vital physiological role in maintaining biomechanical strength and turgor,

allowing for physiological hypertrophy of cardiac tissue during exercise.

Notably, the medial ECM region featured a collagen matrix layer forming particularly large cavities, where localized lipid inclusions were observed (Fig. 3, b). The entire pericardial matrix was uniformly saturated with a small amount of neutral glycosaminoglycans (GAGs). However, acidic GAGs were detected exclusively within the basal membrane structure on the *p. serosum* side of the native pericardium (Fig. 3, c).

Differential elastin staining revealed a small number of elastin fibrils penetrating the entire tissue thickness, with the highest concentration observed on the *p. fibrosum* side (Fig. 3, d).

The ECM of BP-HB group samples exhibited a denser and more compact arrangement of collagen fibers compared to other groups (Fig. 3, a). Notably, extensive fatty inclusions were identified primarily on the *p. fibrosum* side of the tissue (Fig. 3, b).

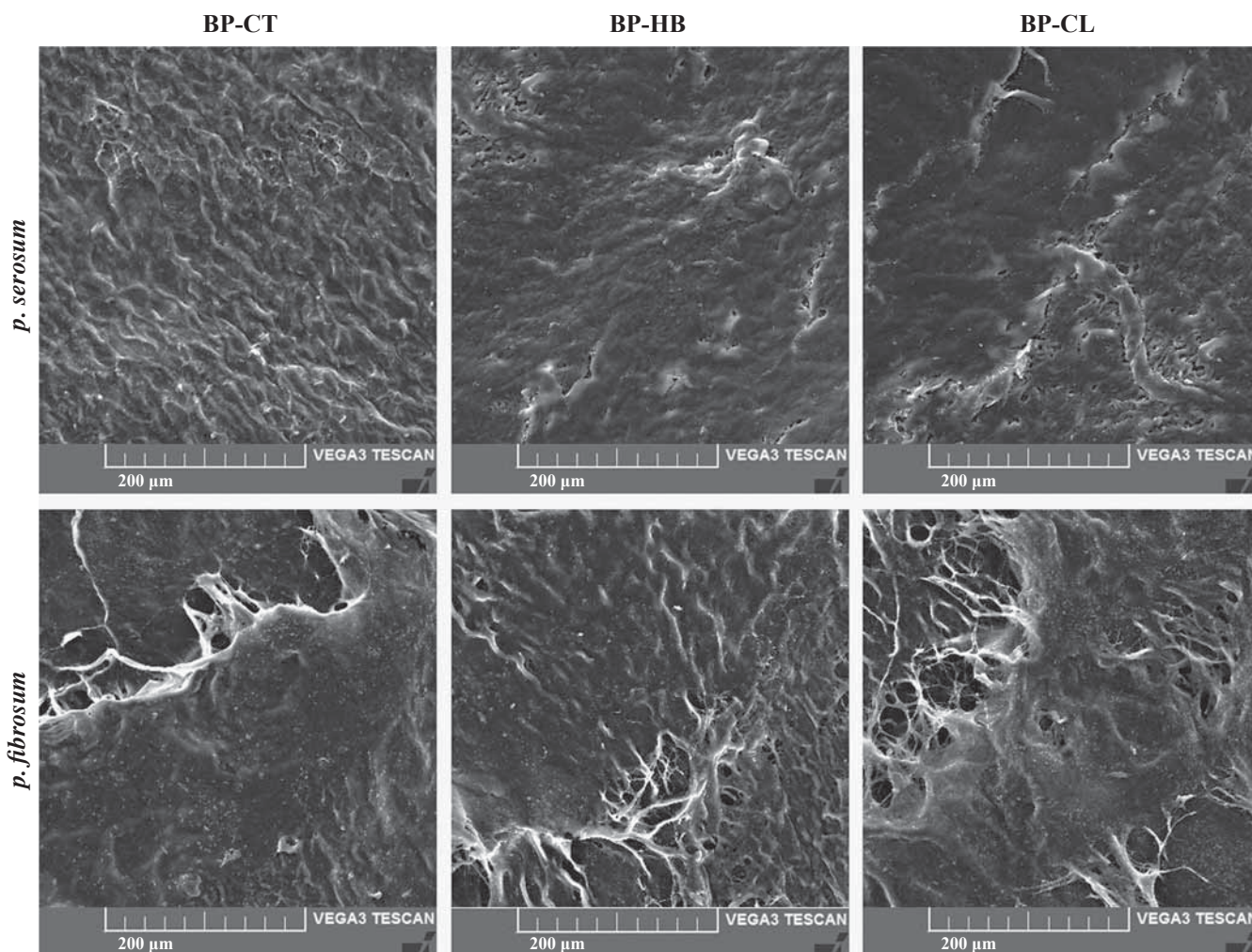


Fig. 2. Surface structure of the *p. serosum* and *p. fibrosum* of bovine pericardium in different tissue areas: core tissue area (BP-CT group), pericardial region at the heart base (BP-HB group) and at the connective ligament base (BP-CL group). Scanning electron microscopy

In addition, the fibrous side showed a higher elastin content, with elastin forming dense strands interwoven between collagen fibers. Furthermore, neutral GAGs were observed in close association with these elastin fibrils (Fig. 3, c, d).

The BP-CL group exhibited a significantly higher content of non-collagenous ECM components. A large number of elastin structures were detected, primarily on the fibrous side, where they were co-localized with neutral GAGs (Fig. 3, c, d). These samples contained abundant lipids within the tissue itself, along with large lipid deposits observed on the surface of the *p. fibrosum* (Fig. 3, b).

Histomorphometric analysis revealed that the BP-CT zone had the most homogeneous and predominantly collagenous composition, with a collagen content of  $95.6 \pm 2.9\%$  (Fig. 4).

The highest elastin and GAG content was observed in the BP-CL group, at  $27.8 \pm 3\%$  and  $17.5 \pm 0.6\%$ , respectively, while the BP-HB group exhibited the highest lipid content, reaching  $21.2 \pm 2.7\%$ .

The lowest cellular density was found in the BP-CT group (Fig. 5, a). DNA quantification further confirmed this, with BP-CT tissue containing  $369.75 \pm 23.12$  ng/mg DNA, which was 1.5 times lower than in the BP-HB group and 2.5 times lower than in the BP-CL group (Fig. 5, b).

Based on these findings, the main pericardial tissue (BP-CT group) is the most suitable for decellularization techniques, as it has the lowest cell and DNA content, allowing for effective immunogenicity suppression while preserving the ECM structure. In addition, the BP-CT group exhibits the most homogeneous ECM composition

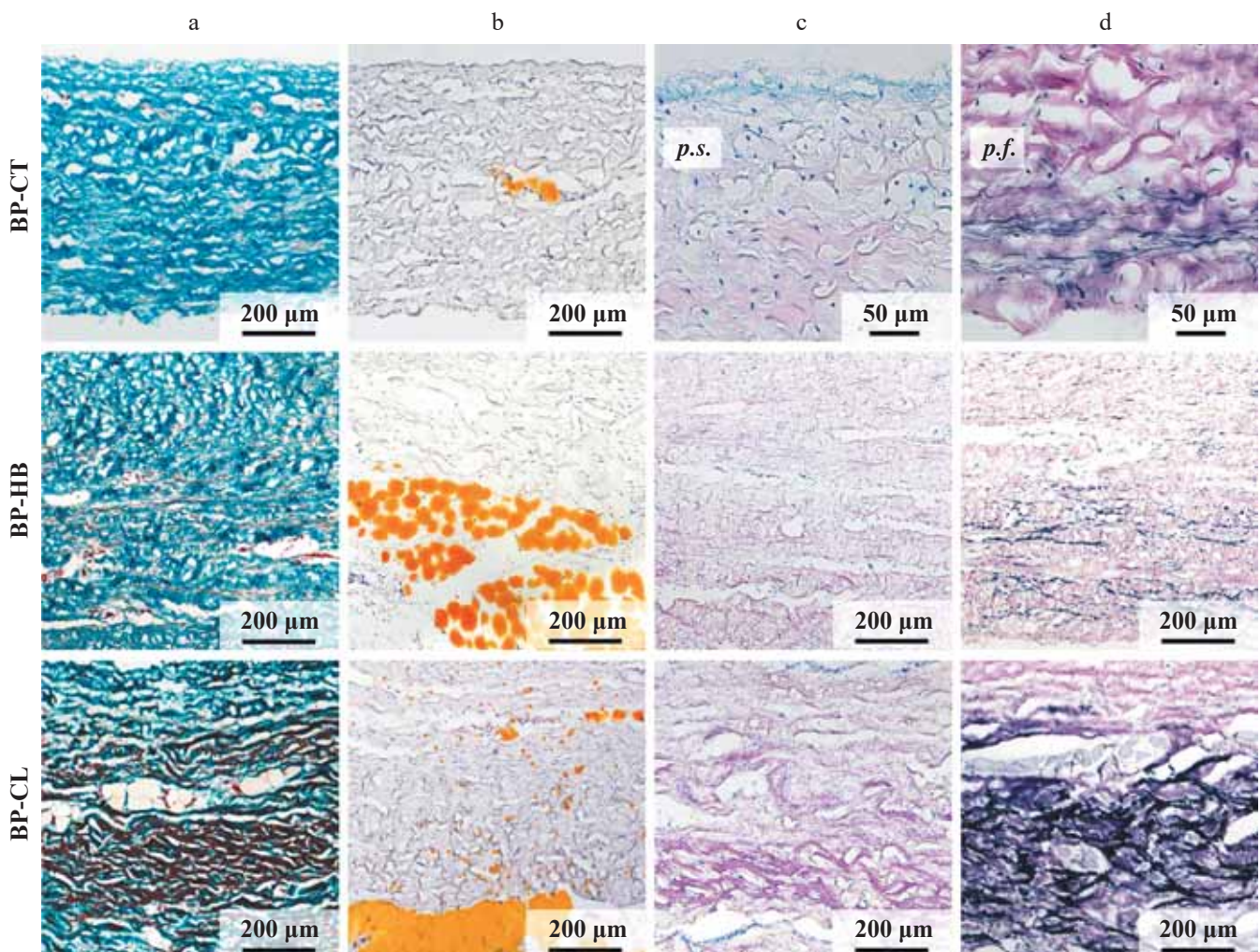


Fig. 3. Structure and composition of bovine pericardium matrix in different tissue areas: core tissue area (BP-CT group), heart base area (BP-HB) and connective ligament base (BP-CL). Light microscopy: a, Lillie's trichrome (collagen – green, non-collagenous components – red-brown); b, Sudan III (lipids – yellow-orange); c, Periodic Acid Schiff-Alcian Blue (acidic GAGs – blue, neutral GAGs – pink); d, Verhoeff–Van Gieson (elastin – black, background – pink). Due to low cellular density and the lowest elastin content in the ECM structure of preparations in the BP-CT group, enlarged fragments are presented for easy perception

on, predominantly collagenous, with low lipid, elastin, and GAG content. This is crucial, as damage to these components during preimplantation processing can trigger calcification and inflammatory responses.

Therefore, the main pericardial tissue (the BP-CT region) is the preferred and safest biomaterial source for manufacturing BHVs and other auxiliary cardiovascular materials, ensuring resistance to calcification and

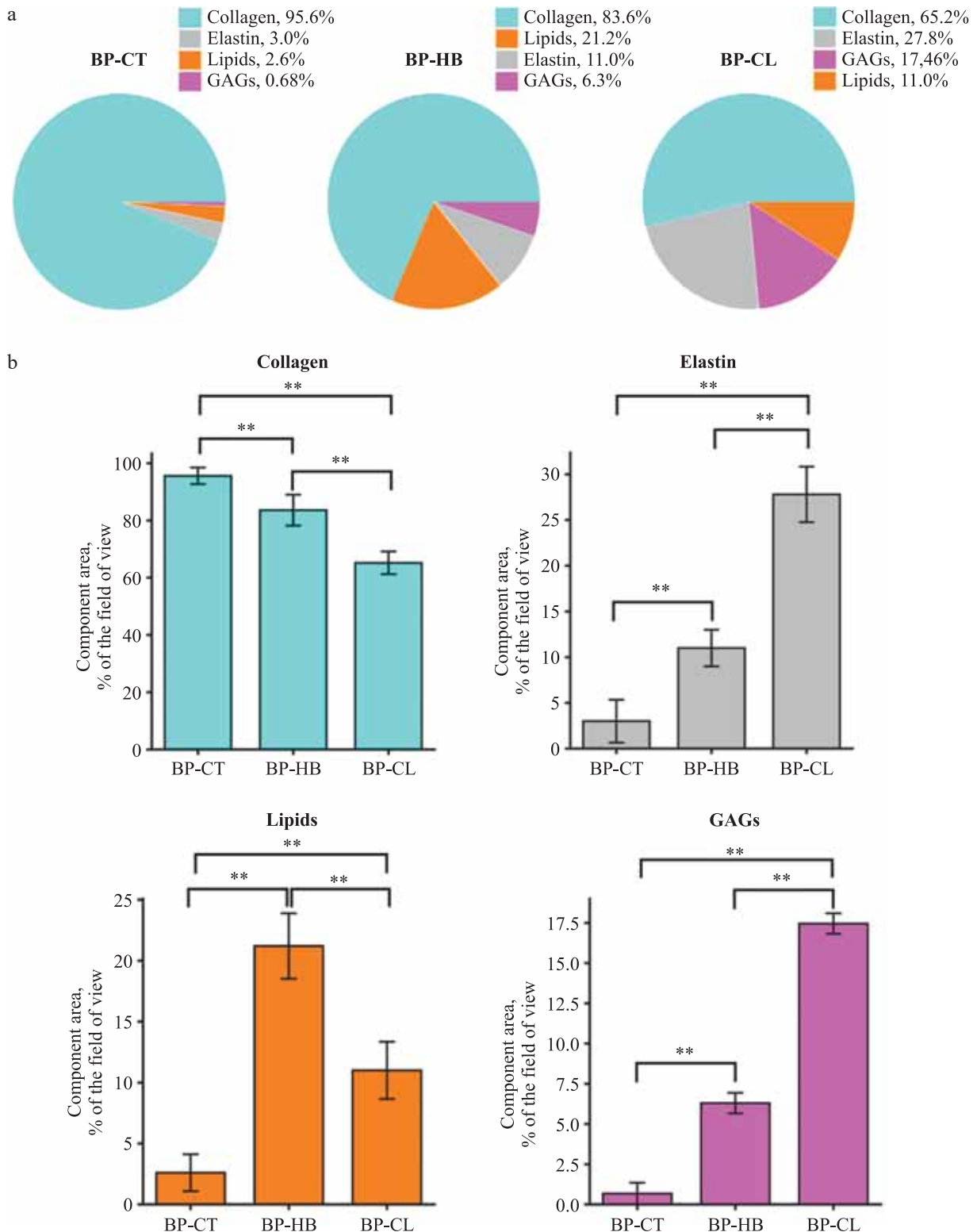


Fig. 4. Results of bioimaging and quantification of histological images of bovine xenopericardium in different topographic areas: core tissue area (BP-CT group), pericardial area at the heart base (BP-HB), connective ligament base area (BP-CL): a, diagrams demonstrating tissue composition; the total percentage of quantified ECM components exceeds 100% owing to the overlap in the color mask areas of co-localized components; b, graphs demonstrating the ratio of components, n = 16, p < 0.01 (Holm–Sidak test)

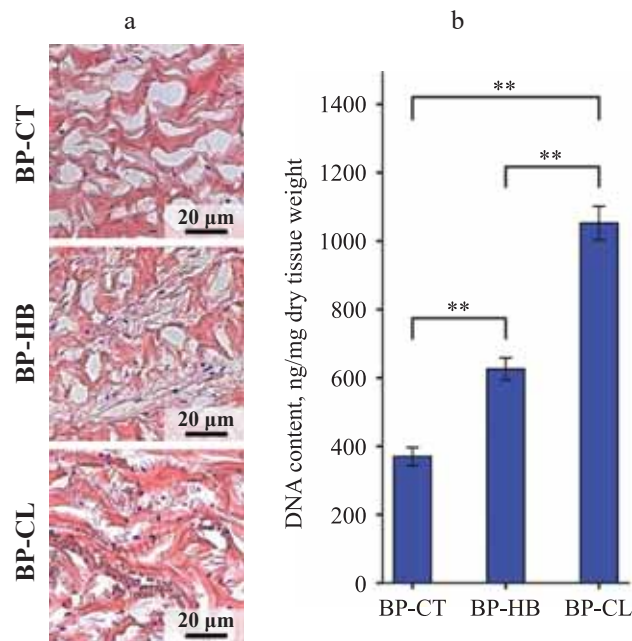


Fig. 5. Cellular composition of bovine pericardium in different tissue areas: core tissue area (BP-CT group), pericardial area at the heart base (BP-HB), connective ligament base area (BP-CL): a, histological images, light microscopy, H&E stain (cell nuclei – purple, matrix components – pink); b, graph showing quantitative DNA content,  $n \geq 5$ ,  $p < 0.01$  (Holm–Sidak test)

degeneration. Meanwhile, the heart base (BP-HB) and connective ligament base (BP-CL), due to their heterogeneity and mineralization potential, are better suited for manufacture of resorbable implants.

## CONCLUSION

The study results highlight the heterogeneous topology of BP across different tissue regions. The high elastin, GAG, and lipid content in certain regions of the pericardium (BP-HB and BP-CL groups) emphasizes the importance of careful tissue selection for biomaterial fabrication, especially for BHVs, which require immunogenic neutrality, calcification resistance, thromboresistance, biostability, biomechanical strength, and re-endothelialization potential.

Given its high ECM homogeneity, stable microarchitecture, minimal immunogenic and proinflammatory components (cells, lipid fractions, and debris), and well-preserved basal lamina (*p. serosum*) – which enhances thromboresistance and re-endothelialization – the xenopericardial core tissue (BP-CT) region is the preferred choice for fabricating BHVs and all other biomaterials in contact with blood and high pressure of systemic blood flow.

Meanwhile, elastin-rich pericardial regions can be repurposed for other reconstructive applications, such as traumatology, orthopedics, and maxillofacial surgery, where their thin, strong, and elastic properties make them ideal for barrier membranes. Additionally, their calci-

fication potential could be leveraged for osteogenesis induction in peri-implant beds.

*The publication of this work was supported by the Russian Science Foundation, Project No. 24-73-10208 “Development of Injectable Calcium Phosphate Hydrated Pastes for Minimally Invasive Administration and Polar Remineralized Composite Barrier Membranes for the Purpose of Targeted Tissue Regeneration in Traumatology and Maxillofacial Surgery”.*

*This paper does not describe any research using humans and animals as subjects.*

*The authors declare no conflict of interest.*

## REFERENCES

- Shklover J, McMasters J, Alfonso-Garcia A, Higuita ML, Panitch A, Marcu L, Griffiths L. Bovine pericardial extracellular matrix niche modulates human aortic endothelial cell phenotype and function. *Sci Rep*. 2019; 9 (1): 16688. doi: 10.1038/s41598-019-53230-1. PMID: 31723198.
- Stieglmeier F, Grab M, König F, Büch J, Hagl C, Thierfelder N. Mapping of bovine pericardium to enable a standardized acquirement of material for medical implants. *J Mech Behav Biomed Mater*. 2021; 118 (3): 104432. doi: 10.1016/j.jmbbm.2021.104432. PMID: 33853036.
- Texakalidis P, Giannopoulos S, Charisis N, Giannopoulos S, Karasavvidis T, Koullias G, Jabbour P. A meta-analysis of randomized trials comparing bovine

- pericardium and other patch materials for carotid endarterectomy. *J Vasc Surg.* 2018; 68 (4): 1241–1256.e1. doi: 10.1016/j.jvs.2018.07.023. PMID: 30244928.
4. Morales MM, Anacleto A, Ferreira Leal JC, Greque VG, Souza AS Jr, Wolosker N. Saccular Superior Vena Cava Aneurysm: Case Report and Comprehensive Review. *Ann Vasc Surg.* 2021; 72: 666.e23–666.e32. doi: 10.1016/j.avsg.2020.10.033. PMID: 33333194.
  5. Bogdanov LA, Osyayev NYu, Bogdanova YuD, Mukhamadiyarov RA, Shabaev AR, Evtushenko AV, Kutikhin AG. Elemental analysis of valvular and atherosclerotic calcification. *Complex Issues of Cardiovascular Diseases.* 2021; 10 (3): 26–33. (In Russ.). doi: 10.17802/2306-1278-2021-10-3-26-33.
  6. Kostyunin AE, Glushkova TV, Lobov AA, Ovcharenko EA, Zaimullina BR, Bogdanov LA et al. Proteolytic Degradation Is a Major Contributor to Bioprosthetic Heart Valve Failure. *J Am Heart Assoc.* 2023; 12 (1): e028215. doi: 10.1161/JAHA.122.028215.
  7. Koziarz A, Makhdom A, Butany J, Ouzounian M, Chung J. Modes of bioprosthetic valve failure: a narrative review. *Curr Opin Cardiol.* 2020; 35 (2): 123–132. doi: 10.1097/HCO.0000000000000711. PMID: 31972604.
  8. Wong ML, Griffiths LG. Immunogenicity in xenogeneic scaffold generation: antigen removal vs decellularization. *Acta Biomater.* 2014; 10: 1806–1816. doi: 10.1016/j.actbio.2014.01.028.
  9. Liu ZZ, Wong ML, Griffiths LG. Effect of bovine pericardial extracellular matrix scaffold niche on seeded human mesenchymal stem cell function. *Sci Rep.* 2016; 6: 37089. doi: 10.1038/srep37089.
  10. Fadeeva IS. The role of recipient cells and tissue matrix structure disorders in the mechanism of calcification of vascular and heart valve transplants: diss. ... Cand. of Biological Sciences. Pushchino, 2013; 158.
  11. Bailey MT, Pillarisetti S, Xiao H, Vyavahare NR. Role of elastin in pathologic calcification of xenograft heart valves. *J Biomed Mater Res A.* 2003; 66 (1): 93–102. doi: 10.1002/jbm.a.10543. PMID: 12833435.
  12. Millán Á, Lanzer P, Sorribas V. The Thermodynamics of Medial Vascular Calcification. *Front Cell Dev Biol.* 2021; 9: 633465. doi: 10.3389/fcell.2021.633465. PMID: 33937234; PMCID: PMC8080379.
  13. Simionescu DT, Lovekamp JJ, Vyavahare NR. Extracellular matrix degrading enzymes are active in porcine stentless aortic bioprosthetic heart valves. *J Biomed Mater Res A.* 2003; 66 (4): 755–763. doi: 10.1002/jbm.a.10066. PMID: 12926026.
  14. Wang X, Zhai W, Wu C, Ma B, Zhang J, Zhang H et al. Procyanidins-crosslinked aortic elastin scaffolds with distinctive anti-calcification and biological properties. *Acta Biomater.* 2015; 16: 81–93. doi: 10.1016/j.actbio.2015.01.028. PMID: 25641644.
  15. Wen S, Zhou Y, Yim WY, Wang S, Xu L, Shi J et al. Mechanisms and Drug Therapies of Bioprosthetic Heart Valve Calcification. *Front Pharmacol.* 2022; 13: 909801. doi: 10.3389/fphar.2022.909801. PMID: 35721165; PMCID: PMC9204043.
  16. Ohri R, Hahn SK, Hoffman AS, Stayton PS, Giachelli CM. Hyaluronic acid grafting mitigates calcification of glutaraldehyde-fixed bovine pericardium. *J Biomed Mater Res A.* 2004; 70 (2): 328–334. doi: 10.1002/jbm.a.30088. PMID: 15227678.
  17. Raghavan D, Simionescu DT, Vyavahare NR. Neomycin prevents enzyme-mediated glycosaminoglycan degradation in bioprosthetic heart valves. *Biomaterials.* 2007; 28 (18): 2861–2868. doi: 10.1016/j.biomaterials.2007.02.017. PMID: 17353047; PMCID: PMC2262162.
  18. Leong J, Munnally A, Liberio B, Cochrane L, Vyavahare N. Neomycin and carbodiimide crosslinking as an alternative to glutaraldehyde for enhanced durability of bioprosthetic heart valves. *J Biomater Appl.* 2013; 27 (8): 948–960. doi: 10.1177/0885328211430542. PMID: 22207605.
  19. Lei Y, Ning Q, Xia Y, Wang Y. Enzyme-oxidative-polymerization method for improving glycosaminoglycans stability and reducing calcification in bioprosthetic heart valves. *Biomed Mater.* 2019; 14 (2): 025012. doi: 10.1088/1748-605X/aafd7c. PMID: 30630147.
  20. Cravedi P, Farouk S, Angeletti A, Edgar L, Tamburrini R, Duisit J et al. Regenerative immunology: the immunological reaction to biomaterials. *Transpl Int.* 2017; 30 (12): 1199–1208. doi: 10.1111/tri.13068. PMID: 28892571; PMCID: PMC6697146.
  21. Ghadially FN. As you like it, Part 3: A critique and historical review of calcification as seen with the electron microscope. *Ultrastruct Pathol.* 2001; 25 (3): 243–267. doi: 10.1080/019131201300343874. PMID: 11465480.
  22. Boskey AL, Posner AS. Extraction of a calcium-phospholipid-phosphate complex from bone. *Calcif Tissue Res.* 1976; 19 (4): 273–283. doi: 10.1007/BF02564010. PMID: 3268.
  23. Neishabouri A, Khaboushan AS, Daghigh F, Kajibafzadeh AM, Zolbin MM. Decellularization in Tissue Engineering and Regenerative Medicine: Evaluation, Modification, and Application Methods. *Front Bioeng Biotechnol.* 2022; 10: 805299. doi: 10.3389/fbioe.2022.805299.
  24. Coscas R, Bensussan M, Jacob MP, Louedec L, Massy Z, Sadoine J et al. Free DNA precipitates calcium phosphate apatite crystals in the arterial wall *in vivo*. *Atherosclerosis.* 2017; 259: 60–67. doi: 10.1016/j.atherosclerosis.2017.03.005.
  25. Glushkova TV, Kostyunin AE. Calcification of bioprosthetic heart valves treated with ethylene glycol diglycidyl ether. *Complex Issues of Cardiovascular Diseases.* 2021; 10 (2): 16–24. (In Russ.). doi: 10.17802/2306-1278-2021-10-2-16-24.
  26. Lilly RD. Pathohistological technique and practical histochemistry. Moscow: MIR, 1969; 645.

The article was submitted to the journal on 20.01.2025